ADVANCED FUNCTIONAL MATERIALS

www.afm-journal.de

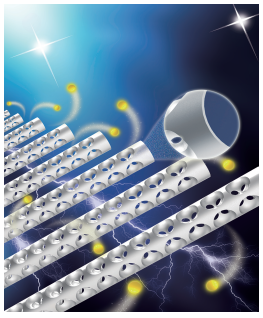

Lithium Ion Batteries

On page 6701, a sustainable route from cheap metallurgical silicon to porous Si/SiO_x nanowires is successfully demonstrated by J. Xiong, C. Yan, and co-workers for high performance lithium ion batteries. With a surface oxide layer of suitable thickness, the huge volume expansion of Si during charge/discharge processes can be greatly accommodated, resulting in superior cycling performance and high reversible capacity.

Graphene Oxide Memory

Al metallic filaments are directly observed in the amorphous top interface layer in Al/graphene oxide (GO)/Al resistive switching memory devices. S.-Y. Choi, J. Y. Lee, H. Y. Jeong, and co-workers also demonstrate, on page 6710, that the oxygen functional groups of graphene oxide are the key elements to explain interface-dominant switching models in GO-based resistive memory.

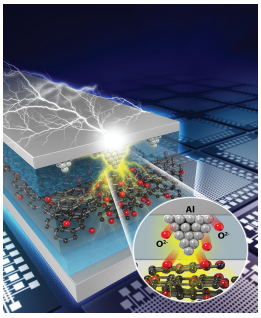

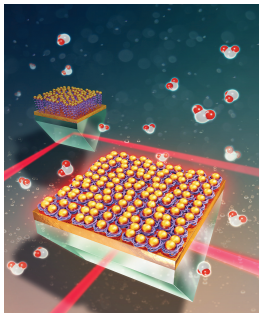

LSPR Coupling

K. Shin, D. H. Kim, and co-workers present, on page 6716, a plasmonic coupling sensing device, comprising AuNPs separated from a Au substrate via a thermoresponsive polymer layer, in a surface plasmon resonance spectrometer configuration. The optical properties of the stimuli-responsive sensing devices are investigated, demonstrating quantified performance with enormous potential in practical bio-sensing and biotechnology applications.

Optical Biosensors

On page 6725, R. Vilensky, M. Bercovici, and E. Segal demonstrate that oxidized porous silicon (PSi) nanostructures can be combined with electrokinetic focusing, allowing significant enhancement of PSi optical biosensors. Embedding a PSi Fabry–Pérot film within a microchannel and implementing on-chip isotachophoresis (ITP) demonstrates label-free DNA detection with 1000-fold improvement in limit of detection of PSi biosensors.

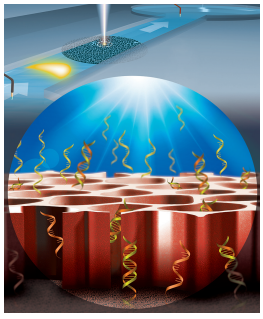

FULL PAPERS

Porous Si/SiO_x nanowires are synthesized by metal-assisted chemical etching of a metallurgical silicon feedstock followed by a postannealing process. The oxide layer with appropriate thickness is able to accommodate the huge volume expansion of underlying Si, thus enhancing electrochemical performance. Therefore, an average of only 0.04% drop per cycle is recorded in a prolonged test of 560 cycles.

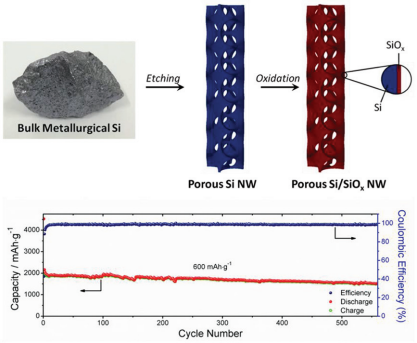

Lithium Ion Batteries

Conducting nanofilaments are clearly characterized in the top interface layer formed by the chemical reaction between the top electrode and graphene oxide layer in graphene-oxide-resistive switching memory. The migration of oxygen ions from the interface layer to graphene oxide layer makes nanosized Al filaments. Oxygen functional groups of graphene oxide are the key elements to reveal resistive switching mechanisms within graphene-oxide-based memory.

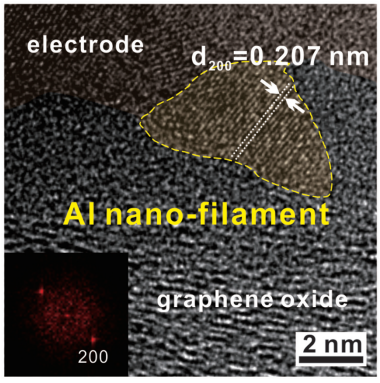

Graphene Oxide Memory

A plasmonic coupling sensing device is designed, comprising AuNPs separated from the Au substrate in a surface plasmon resonance (SPR) spectrometer through a thermoresponsive polymer layer. The optical properties of the stimuli-responsive sensing devices are investigated by in situ and scan-mode SPR analysis. The Au film-PNIPAM-AuNP system shows markedly enhanced sensitivity toward refractive index sensing due to SPR coupling.

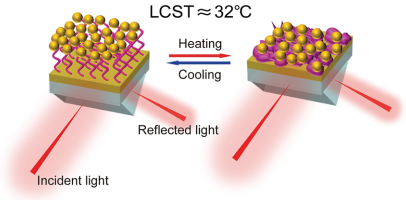

LSPR Coupling

1000-fold sensitivity enhancement of porous Si (PSi) biosensors for nucleic acid detection is achieved by a novel label-free assay that interfaces PSi Fabry–Pérot interferometry with isotachophoresis. The presented concepts can be readily applied to other ionic targets, paving way for the development of other highly sensitive chemical and biochemical assays.

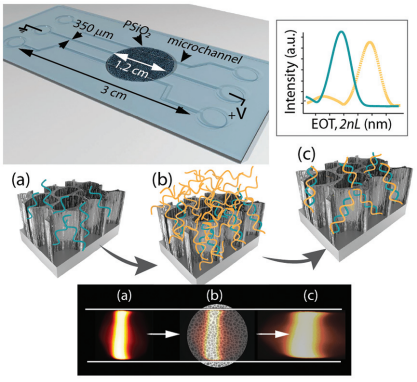

Optical Biosensors

CONTENTS

FULL PAPERS

Kesterite Solar Cells

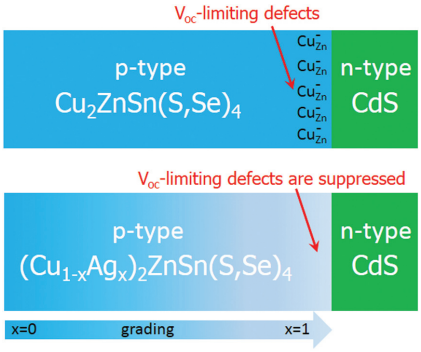

A new strategy is proposed to overcome the V_{oc} bottleneck and increase the efficiency of the kesterite solar cells. This is achieved by forming composition-graded $(Cu_{1-x}Ag_x)_2ZnSn(S,Se)_4$ alloys as the absorber layer.

Drug Delivery

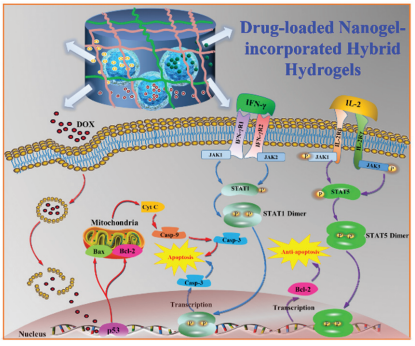

Nanostructured physical and chemical hybrid hydrogels can retain drug activity for a long time and represent a novel class of local delivery carriers for cancer treatment. The active components produce cooperative cytostatic and cytocidal effects on the tumor cells by combining the effects of three different apoptosis-related Janus kinase/signal transducer and activator of transcription (JAK/STAT) and mitochondrial pathways.

3D Printing

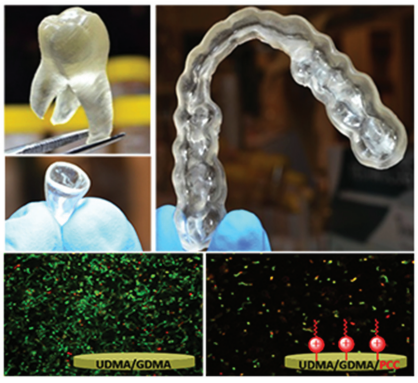

Development of 3D printable, bacterial contact-killing resins is acheived by incorporating positively charged compounds into the stereolithography-compatible composite resins. Complex geometries of oral appliances bearing antimicrobial functions have been successfully printed and the mechanical properties of 3D printed objects are almost identical to conventionally photocured polymer samples, which implies potential applications in clinical use.

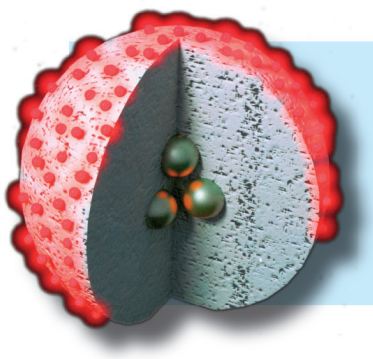

How to contact us:

Editorial Office:
Phone: (+49) 6201-606-286/531
Fax: (+49) 6201-606-500
Email: afm@wiley-vch.de

Reprints:
cherth@wiley-vch.de

Copyright Permission:
Fax: (+49) 6201-606-332
Email: rights@wiley-vch.de

FULL PAPERS

A novel approach to evoke aligned wrinkling in thin film systems is presented. By the interaction of a ferromagnetic thin film with a tailored micromagnetic stray field pattern the systems entropy can be influenced as shown by proof of principle experiments. Using additional external magnetic stimuli this method allows switchable wrinkle systems.

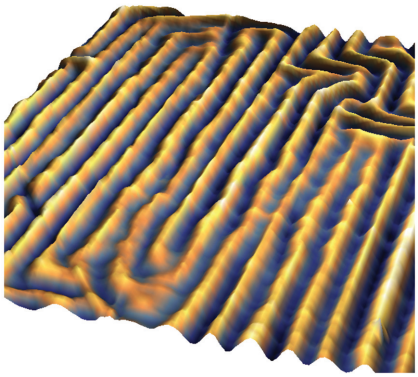

Thin Films

Selective Alignment of Molecular Glass Wrinkles by Engineered Magnetic Field Landscapes

Multifunctional materials are synthesized for electrochemical capacitor electrodes through surface functionalization of the active material by covalent attachment of organic moieties. The attached species can serve two purposes: provide mechanical stability by favoring self-adhesion of the active material particles, thus avoiding the electrochemically inactive binder in the electrode formulation and provide better interaction of the electrode with the ions of the electrolyte.

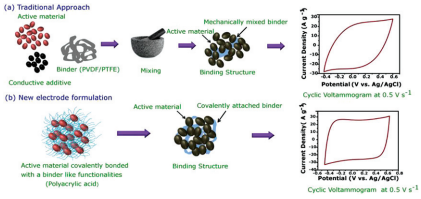

Electrochemical Capacitors

Multifunctional Carbon for Electrochemical Double-Layer Capacitors

A high quantum efficiency of 20% in blue, solution-processed, thermally activated delayed fluorescent devices is achieved by developing blue emitters with an F functional unit instead of CN functional unit.

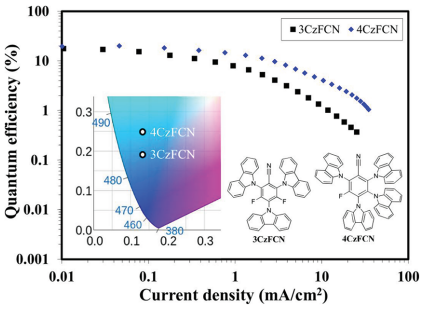

Fluorescent Devices

20% External Quantum Efficiency in Solution-Processed Blue Thermally Activated Delayed Fluorescent Devices

Dark-colored rutile TiO_2 ultrafine nanorods doped by Ti^{3+} are proposed as a superior anode for Li-ion batteries featuring remarkable high-rate capabilities and cycling stabilities, because of a promoted electron transport by Ti^{3+} and a shortened Li^+ diffusion length. Outstanding reversible capacities of 111.7 mAh g^{-1} at 20 °C and 93.6 mAh g^{-1} at 50 °C are achieved.

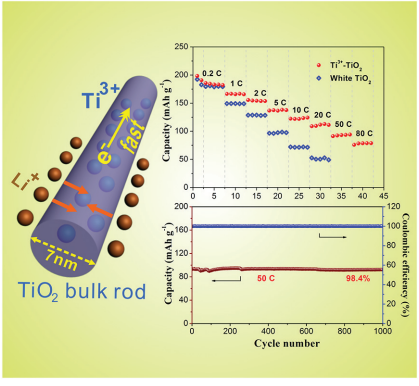

Lithium-Ion Batteries

Ti^{3+} Self-Doped Dark Rutile TiO_2 Ultrafine Nanorods with Durable High-Rate Capability for Lithium-Ion Batteries

FULL PAPERS

Hole Transport

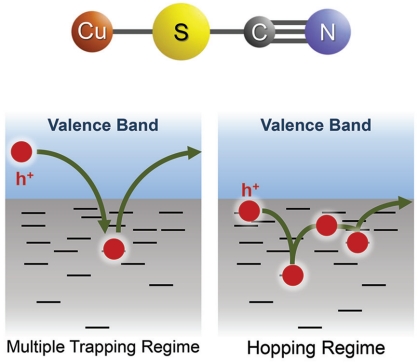

The wide bandgap p-type semiconductor copper(I) thiocyanate (CuSCN) has the potential to replace conventional hole-transport materials in numerous opto/electronics applications. This work provides a comprehensive analysis of the charge transport properties of solution-processed CuSCN layers. Various techniques are employed to evaluate the dielectric constant, flat-band voltage, unintentional doping concentration, density of states in the mobility gap, and hole-transport mechanisms.

Hydrogen Evolution

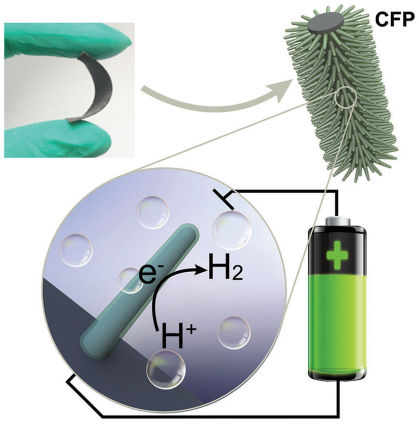

Nanostructured $NiCo_2O_4$/CuS heterostructure nanowires coated on a carbon fiber paper are fabricated as a self-standing 3D hydrogen evolution cathode. Benefitting from their structural merits including enhanced overall conductivity and rich effective active sites, this electrode shows exceptional high HER performance and excellent durability in acid medium, better than any noble metal free electrocatalyst reported to date.